Title page

Convergent and discriminant validity of default mode network and limbic network perfusion in amnestic mild cognitive impairment patients

Giulia Quattrini[1,2], Moira Marizzoni[1,3], Francesca B Pizzini[4], Ilaria Boscolo Galazzo[5], Marco Aiello[6], Mira Didic[7,8], Andrea Soricelli[6,9], Diego Albani[10], Melissa Romano[1], Olivier Blin[11], Gianluigi Forloni[10], Xavier Golay[12], Jorge Jovicich[13], Pradeep J Nathan[14], Jill C Richardson[15], Marco Salvatore[8], Giovanni B Frisoni[1,16], Michela Pievani[1*], on behalf of the PharmaCog Consortium.

[1] Laboratory of Alzheimer's Neuroimaging and Epidemiology (LANE), IRCCS Istituto Centro San Giovanni di Dio Fatebenefratelli, Brescia, Italy;

[2] Department of Molecular and Translational Medicine, University of Brescia, Brescia, Italy;

[3] Laboratory of Biological Psychiatry, IRCCS Istituto Centro San Giovanni di Dio Fatebenefratelli, Brescia, Italy;

[4] Radiology, Department of Diagnostic and Public Health, University of Verona, Verona, Italy;

[5] Department of Computer Science, University of Verona, Verona, Italy;

[6] IRCCS SDN, Napoli;

[7] Aix-Marseille Univ, INSERM, INS, Instit Neurosci des Syst, Marseille, France;

[8] APHM, Timone, Service de Neurologie et Neuropsychologie, Hôpital Timone Adultes, Marseille, France;

[9] Department of Sport Sciences University of Naples Parthenope

[10] Neuroscience Department, Istituto di Ricerche Farmacologiche Mario Negri IRCCS, Milano, Italy;

[11] Aix-Marseille Univ, INSERM, INS, Instit Neurosci des Syst, DHUNE, Ap-Hm, Marseille, France;

[12] Department of Brain Repair and Rehabilitation, University College London, Institute of Neurology, London, England;

[13] Center for Mind/Brain Sciences - CIMeC, University of Trento, Rovereto, Italy;

[14] Department of Psychiatry, University of Cambridge, UK;

[15] Neurosciences Therapeutic Area, GlaxoSmithKline R&D, Gunnels Wood Road, Stevenage, United Kingdom;

[16] Memory Clinic and LANVIE-Laboratory of Neuroimaging of Aging, University Hospitals and University of Geneva, Geneva, Switzerland.

***Corresponding author:**

Michela Pievani, PhD

Laboratory Alzheimer's Neuroimaging & Epidemiology

IRCCS Istituto Centro San Giovanni di Dio Fatebenefratelli

via Pilastroni 4, 25125 - Brescia, Italy

email: mpievani@fatebenefratelli.eu

Running title: Brain perfusion and AD features in aMCI

Abstract

Background. Previous studies reported default mode network (DMN) and limbic network (LIN) brain perfusion deficits in patients with amnestic mild cognitive impairment (aMCI), frequently a prodromal stage of Alzheimer's disease (AD). However, the validity of these measures as AD markers has not yet been tested using MRI arterial spin labeling (ASL).

Objective. To investigate the convergent and discriminant validity of DMN and LIN perfusion in aMCI.

Methods. We collected core AD markers (amyloid-β 42 [$A\beta_{42}$], phosphorylated tau 181 levels in cerebrospinal fluid [CSF]), neurodegenerative (hippocampal volumes and CSF total tau), vascular (white matter hyperintensities), genetic (apolipoprotein E [APOE] status), and cognitive features (memory functioning on Paired Associate Learning test [PAL]) in 14 aMCI patients. Cerebral blood flow (CBF) was extracted from DMN and LIN using ASL and correlated with AD features to assess convergent validity. Discriminant validity was assessed carrying out the same analysis with AD-unrelated features, i.e. somatomotor and visual networks' perfusion, cerebellar volume, and processing speed.

Results. Perfusion was reduced in the DMN (F=5.486, p=0.039) and LIN (F=12.678, p=0.004) in APOE ε4 carriers compared to non-carriers. LIN perfusion correlated with CSF $A\beta_{42}$ levels (r=0.678, p=0.022) and memory impairment (PAL, number of errors, r=-0.779, p=0.002). No significant correlation was detected with tau, neurodegeneration, and vascular features, nor with AD-unrelated features.

Conclusion. Our results support the validity of DMN and LIN ASL perfusion as AD markers in aMCI, indicating a significant correlation between CBF and amyloidosis, APOE ε4, and memory impairment.

Keywords: Mild cognitive impairment, arterial spin labeling, brain perfusion, limbic network, default mode network, Alzheimer's disease.

INTRODUCTION

Amnestic mild cognitive impairment (aMCI) denotes a clinical syndrome characterized by cognitive deficits in the context of preserved activities of daily living and can represent a prodromal stage of Alzheimer's disease (AD) [1]. Individuals with aMCI due to AD present abnormalities in AD biomarkers years prior to symptom onset, including abnormal accumulation of amyloid-beta (Aβ) and tau proteins and neurodegeneration [2,3], which are key pathological processes in the AD cascade [4,5]. However, other processes are also thought to play a role in the disease pathogenesis, such as vascular dysfunction [6].

Vascular dysfunction can be assessed in vivo using arterial spin labelling (ASL), a non-invasive magnetic resonance imaging (MRI) technique that measures brain perfusion, i.e. the nutrients' and oxygen supply through the cerebral blood flow (CBF) using the arterial blood water as endogenous tracer [7,8]. Brain hypoperfusion can be observed early in the progression of AD, i.e. from prodromal stages [9], in the precuneus/posterior cingulate cortex, inferior parietal lobe, anterior cingulate cortex, hippocampus, medial and lateral temporal cortex, inferior and medial frontal gyri [10-16] Importantly, these areas correspond to hubs of functional networks affected in AD, i.e. the default mode network (DMN) and the limbic network (LIN) [17-19]. DMN and LIN impairment is widely documented in aMCI [20-22], and DMN and LIN areas might be the earliest sites of AD pathological changes, i.e. amyloid and tau accumulation [23-26]. Moreover, damages to these networks are clinically relevant being linked to memory retrieval and autobiographical memory (DMN), semantic memory, behavior, and item recognition memory (LIN), which are typically impaired in aMCI and AD [27-29].

While some studies suggest that ASL may be a promising marker for AD diagnosis [30], early detection [31], monitoring of disease progression and conversion from aMCI to AD [32,33], no study

has yet assessed whether CBF changes in the DMN and LIN may represent valid AD markers. The assessment of perfusion convergent and discriminant validity can provide important information on its clinical validity and thus utility. Convergent validity can be assessed by investigating the association with core AD markers / features and discriminant validity through associations with AD unrelated features. Current evidence for the convergent validity of perfusion measures in aMCI is provided by studies reporting an association between single photon emission computed tomography (SPECT) and ASL CBF level in areas of the DMN and/or LIN and Aβ accumulation [34-36], tau burden [37] and longitudinal tau deposition [38], and cortical atrophy in the medial temporal lobe [39] Previous studies also reported an association between episodic memory decline and hypoperfusion in the middle frontal cortex and anterior cingulate cortex [33,40] (DMN hubs). When considering genetic risk factors for AD, some ASL reports revealed a relationship between CBF and apolipoprotein E (APOE) ε4 allele, although the direction of these associations is conflicting [41,42]. Finally, increasing vascular burden has also been associated with hypoperfusion in ASL or SPECT studies [16,39].

Discriminant validity can be assessed by investigating features that have been described as relatively unimpaired or affected in later in AD. For example, sensorimotor, visual, and cerebellar areas are among the last brain regions affected by amyloid and tau [24], and by functional, structural and metabolic dysfunctions [43,44]. At the cognitive level, visuo-spatial and executive functions are affected later than memory [45], congruently with pathology spread to the neocortex.

The aim of the present study was to investigate in aMCI patients the convergent and discriminant validity of ASL perfusion in DMN and LIN networks. To test the convergent validity, we selected: (i) genetic risk factors (APOE ε4 status); (ii) core pathological features (Aβ and p-tau); (iii) neurodegenerative features (hippocampal volumes and total tau); (iv) neuropsychological features

(episodic memory); and (v) vascular burden (white matter lesions). For discriminant validity, we selected two unrelated features (i.e., volume of the cerebellum and non-memory cognitive functions) and two unrelated networks (i.e., sensorimotor [SMN] and visual [VIS] networks).

MATERIALS AND METHODS

PARTICIPANTS

Subjects were enrolled in the PharmaCog - WP5/European ADNI project (https://www.alzheimer-europe.org/Research/PharmaCog). Briefly, participants underwent a baseline assessment and follow-up examinations every 6 months for at least 2 years or until patient progressed to clinical dementia. Each assessment included a clinical and cognitive evaluation, and MRI exam. Cerebrospinal fluid (CSF) sampling was performed at baseline and after 18 months. ASL was included later in the study, starting from month 24 (T24). Therefore, for the present study we included only subjects evaluated at T24 who had not yet converted to dementia. The initial cohort included 16 aMCI, which were recruited from Marseille (n = 3), Brescia (n = 8), and Naples (n = 5). Two subjects were subsequently excluded due to MRI issues (see section "ASL processing"), leading to a final sample of 14 aMCI. Inclusion and exclusion criteria, clinical and neuropsychological assessment have been previously described [46].

The study was approved by the local ethical committees or institutional review boards of the participating institutions, and all subjects provided written informed consent prior to participation in the study.

MRI

MRI ACQUISITION

All MRI scans were performed on 3T Siemens machines (Siemens Verio for Marseille, Siemens Allegra for Brescia, and Siemens Biograph mMR for Naples), and only vendor-provided sequences were used. The MRI protocol included anatomical 3D T1-weighted (T1-w), 2D T2*-weighted, 2D T2-weighted-fluid-attenuated inversion recovery (FLAIR), resting-state functional MRI, diffusion tensor imaging, and 2D ASL sequences. For the aim of this study, we analyzed only the ASL, 3D T1-w, and 2D T2 FLAIR scans. ASL MRI protocols were harmonized choosing the same sequence type (pulsed ASL PICORE Q2TIPS, 2D gradient-echo EPI) and optimizing all the relevant sequence parameters (TR, TE, inversion times , flip angle, number of measurements, number of slices, and voxel size), with minimal variations across sites. A calibration scan (M0) with the same parameters as the corresponding ASL sequence but longer repetition time (10 s) was also acquired to estimate the equilibrium magnetization of arterial blood. For 3D T1-w, the harmonization procedure has been previously described [47]. The parameters of all the acquired images were automatically checked for their compliance with the harmonized protocol by M. R. using in-house scripts. The Supplementary Table 1 summarizes the scanner and sequences' details.

MRI PROCESSING

ASL PROCESSING

Due to excessive motion during the acquisitions, two subjects were excluded leading to a final sample of 14 aMCI patients. ASL data were preprocessed and analyzed using FMRIB Software Library (FSL) v5.0.9. Data were first realigned to account for movement artefacts and then corrected for nuisance effects using the 6 head motion profiles plus the mean white matter and CSF signals in a linear

regression. In addition, the coregistration parameters from ASL space to individual T1-w were estimated using the M0 calibration scan as reference image (rigid-body registration with 6 degrees of freedom [DOF] and boundary-based registration [BBR] cost function). Each T1-w image was also normalized to the 2-mm Montreal Neurological Institute (MNI) standard space using a non-linear method (FMRIB's nonlinear image registration tool [FNIRT], https://fsl.fmrib.ox.ac.uk/fsl/fslwiki/FNIRT).

Pre-processed control and label volumes were pair-wise subtracted and averaged to obtain perfusion-weighted images, which were quantified into CBF (ml/100g/min) applying the general kinetic model [48]and following the white paper recommendations [49].

Partial volume corrected (PVC) CBF maps were also created for each subject. In detail, tissue probability maps derived from the segmentation of the individual T1-w were first smoothed to mimic the ASL resolution. These smoothed maps were then downsampled to the ASL space using the inverse of the previously estimated transformation matrix and applied to calculate the PVC CBF maps according to a previously described procedure [50]. Finally, each CBF map was spatially normalized using the joint ASL/T1-w and T1-w/MNI space transformation parameters.

We selected the DMN and the LIN as networks of interest (NOIs) for AD related networks, while the SMN and the VIS were included for AD unrelated networks. The Schaefer parcellation (7 resting-state functional MRI networks and 100 parcels, 2 mm resolution) [51]was used to derive the masks of the NOIs.

3D T1-W PROCESSING

All T1-w scans underwent a visual quality check[52], performed by a 5-year experienced investigator (G. Q.), and were then processed using the cross-sectional pipeline of FreeSurfer v6.0 [53,55] (https://surfer.nmr.mgh.harvard.edu/). The standard procedure includes the motion and non-uniformity corrections, skull stripping, linear and non-linear Talairach transformations from native to MNI305 standard space, intensity normalization, white matter and deep structures segmentation, gray/white matter boundary tessellation, topology correction, and surface deformation to derive the brain white and outer (pial) surfaces according to the grey/white matter intensity gradients. Several deformable procedures are then implemented to create surface-based data, including the cortex parcellation according to gyri and sulci. All outputs were visually inspected (G. Q.), and none required manual editing.

Hippocampal and cerebellar cortex volumes were selected as AD related and unrelated features, respectively. Volumes were averaged across hemispheres and corrected for the total intracranial volume (ICV) automatically extracted by FreeSurfer.

2D T2 FLAIR PROCESSING

Vascular burden (AD-related feature) was estimated using the total volume of white matter hyperintensities (WMHs) on FLAIR images. The lesion prediction algorithm (LPA) [56,57], as implemented in the Lesion Segmentation Tool (LST) toolbox (version 2.0.15; https://www.statistical-modelling.de/lst.html) for the Statistical Parametric Mapping (SPM) 12 (https://www.fil.ion.ucl.ac.uk/spm/software/spm12/) tool, was used to segment WMHs. The respective 3D T1-w image was used as reference image for the coregistration before lesions' segmentation. Lesion probability maps were then binarized after applying a standard threshold $\kappa > 0.95$. For each

subject, the total WMHs volume was calculated by LPA, and then corrected for the ICV computed with FreeSurfer.

APOE GENOTYPING

APOE genotyping (AD-related feature) was performed at the Mario Negri Institute of Milan. The genomic DNA (gDNA) was extracted from whole blood with a dedicated kit (Promega, Madison, WI, USA) and its quality and quantity was assessed by UV 260/280 measure while integrity was assessed by agarose gel electrophoresis. A real-time polymerase chain reaction (RT-PCR) with TaqMan technology (Life Technologies, Carlsbad, CA, USA) was then performed on about 50 ng gDNA. The instrument's software automatically performed showed the genotype calling, which was finally visually checked through the generated fluorescence plots.

CSF BIOMARKERS

The CSF was collected at the baseline and at the third timepoint of the PharmaCog study, thus we included the closest timepoint available (18 months) for comparisons with ASL data. The CSF samples were pre-processed, frozen, and centrally stored at the Mario Negri Institute of Milan, following the recommendation coming from the Alzheimer's Association Quality Control Programme for CSF biomarkers [58]. The quantification of CSF levels of $A\beta_{42}$, t-tau and p-tau at residue 181 (AD related features) was performed using the single-parameter colorimetric enzyme-linked immunosorbent assay (ELISA) kits (Innogenetics, Belgium). A sigmoidal standard curve was plotted to allow the quantitative expression (pg/mL) of measured 450 nm light absorbance. Lower CSF levels of $A\beta_{42}$ are considered mirror of higher levels of cerebral amyloid plaques, while higher CSF levels of p-tau and t-tau are indicative of greater cerebral tau pathology and neuronal injury [4].

COGNITION

The complete clinical and cognitive evaluation has been described elsewhere [46]. Briefly, participants underwent a cognitive (Mini-mental state examination and Alzheimer's disease assessment scale-Cognitive subscale), functional (Functional assessment questionnaire), mood and behavior (Geriatric depression scale) assessment and a complete multidomain neuropsychological evaluation using the Cambridge Neuropsychological Test Automated Battery (CANTAB; https://www.cambridgecognition.com/cantab/) [46]. For this study, the number of errors at the Paired Associated Learning Test (PAL) was selected as a measure of episodic memory (AD-related feature). The reaction time at the Reaction Time (RTI) test was included as a measure of attention and processing speed (AD-unrelated feature) [59].

STATISTICAL ANALYSIS

Statistical analyses were performed using IBM SPSS Statistics for Windows, version 23. The Partial correlation was used to test the correlation between CBF and AD core pathophysiological (CSF $A\beta_{42}$ and p-tau levels), neurodegeneration (CSF t-tau levels, hippocampal and cerebellar volumes), and cognitive (episodic memory and processing speed) feature, and vascular burden (total WMHs volume), meanwhile controlling for scanner effects. For genetic features, CBF measures were compared between APOE ε4 carriers (ε4+) and APOE Ɛ4 non-carriers (ε4-) using the General Linear Model (ANCOVA). The same analyses were conducted to test correlation between the CBF of SMN and VIS and AD-related and unrelated features, and to compare ε4+ *vs* ε4-. MRI site was included as a covariate in all the analyses to correct for potential scanner-related differences. These comparisons were assessed at an uncorrected threshold of $p < 0.05$. In addition, the results were also assessed after multiple comparisons correction with Bonferroni (correcting for AD-related features to avoid type 1 error, $n = 7$; $p < 0.007$).

RESULTS

CLINICAL, DEMOGRAPHIC, AND GENETIC FEATURES

Table 1 summarizes the clinical and demographic features of aMCI subjects. More than half of patients were ε4+ (57%) and had prodromal AD (58%) (i.e., AD-like $A\beta_{42}$/p-tau ratio based on established cut-offs depending on APOE ε4 status [60]). Moreover, all subjects with clinical follow-up available (n = 10) converted to dementia. The complete neuropsychological assessment included in the PharmaCog assessment is shown for descriptive purposes in the Supplementary Table 2.

CONVERGENT AND DISCRIMINANT VALIDITY NETWORKS' PERFUSION

Table 2 summarizes the values of networks' CBF and of AD-related and unrelated features.

CONVERGENT VALIDITY

Compared to ε4-, ε4+ had lower perfusion in the DMN ($p = 0.039$; Figure 1) and LIN ($p = 0.004$; Figure 2). However, only the latter survived multiple comparisons correction. Concerning AD pathophysiological markers, CSF $A\beta_{42}$ levels showed a positive association with CBF levels of the LIN ($r = 0.678$, $p = 0.022$; Figure 2), which did not survive multiple comparisons correction. As *post-hoc* analysis, an effect of the APOE ε4 allele on CSF $A\beta_{42}$ levels was also observed (CSF $A\beta_{42}$: 492 ± 111 vs 959 ± 149 pg/ml in ε4+ vs. ε4-; $F = 38.120$, $p < 0.001$).

No significant correlation emerged with the CBF of the DMN ($p > 0.050$; Figure 1). Similarly, no association was detected between CSF p-tau levels and CBF of the DMN (Figure 1) nor the LIN (Figure 2) ($p > 0.050$). As regards neurodegeneration markers, CSF t-tau levels and hippocampal

volume were not significantly associated ($p > 0.050$) with CBF in the DMN (Figure 1) or the LIN (Figure 2). Episodic memory impairment (PAL, number of errors) was negatively associated to CBF levels within the LIN ($r = -0.779$, $p = 0.002$; Figure 2). This association survived multiple comparisons correction. A *post-hoc* test for the association between episodic memory impairment and CSF markers showed a correlation with $A\beta_{42}$ ($r = -0.713$, $p = 0.011$) but not with p-tau ($r = 0.333$, $p = 0.317$). Moreover, the episodic memory impairment was different between ε4+ (number of errors: 94 ± 37) and ε4- (76 ± 27) ($F = 6.466$, $p = 0.027$). No association ($p > 0.050$) was detected with CBF in the DMN (Figure 1). Finally, WMHs volume did not show any significant association ($p > 0.050$) with CBF within DMN (Figure 1) or LIN (Figure 2).

DISCRIMINANT VALIDITY

No significant association was detected between CBF in the DMN and LIN and AD-unrelated features (i.e., cerebellar atrophy and processing speed; $p > 0.050$; Figures 1 - 2).

Moreover, no association was detected between CBF in AD-unrelated networks and AD features ($p > 0.050$; Supplementary Figures 1 - 2).

DISCUSSION

In this study, we investigated the validity of ASL perfusion as possible AD marker in aMCI, assessing the convergent and discriminant validity of CBF within two AD-related networks (DMN and LIN). In line with our hypotheses, the convergent validity was supported by significant associations with several AD features, while the lack of association between perfusion and AD-unrelated features / networks

supported their discriminant validity. Taken together, these results show the promise of networks' perfusion as an AD marker in aMCI patients.

Convergent validity was supported by the significant association of CBF with 3 out of 5 AD-related features (APOE ε4 allele, amyloidosis, and memory). Notably, the observation of significant associations with APOE ε4 allele and Aβ load, but not with tau, neurodegeneration and vascular features, suggests a link between perfusion and upstream, but not downstream, AD processes[4]. The finding of lower DMN and LIN perfusion in ε4+ compared to ε4- is in line with the study of Wierenga and colleagues [41] that reported lower CBF in ε4+, mapping to the parahippocampal and fusiform gyri (DMN and LIN temporal regions). Other previous reports on the effect of APOE genotype on perfusion found mixed results [10,41,42,61]; however, none specifically focused on AD-related circuits. The regional specificity of our findings is also corroborated by the relative sparing of AD unrelated networks (SMN and VIS). Preclinical data suggest that APOE ε4 may have a role in neurovascular dysfunction, promoting inflammatory processes that, in turn, increase the bloodbrain barrier permeability (BBB) to breakdown and disrupt microvascular integrity, especially in the hippocampal and parahippocampal regions (core DMN areas) [62,63]. The association between LIN hypoperfusion and amyloidosis is in line with previous studies reporting lower CBF in the entorhinal cortex [36] and inferior temporal gyrus [34,36] of aMCI with higher Aβ load. LIN areas (orbitofrontal, entorhinal and anterior temporal) are among the first regions affected by amyloid deposition (Braak stage A [24]), while DMN core areas (hippocampus and precuneus) are affected slightly later (Braak stage B [24]), thus providing a possible explanation for lack of association between CBF and amyloidosis in the DMN, which is consistently reported in MCI [11-16]. However, we cannot exclude that this null result could be related to some methodological differences or limitations of our design, such as the usage of a measure lacking spatial specificity (i.e., CSF), the 6-month gap between CSF and MRI acquisition, or

the small sample size. Notably, the association between Aβ and LIN hypoperfusion may be explained by other mechanisms than a direct effect of Aβ on perfusion. For example, this relationship may be primarily driven by the presence of APOE ε4 allele. Indeed, the presence of APOE ε4 allele is associated with amyloidosis [64], an effect we observed also in our sample. Thus, the association between LIN hypoperfusion and amyloidosis may be the indirect result of a pathological cascade initiated by APOE ε4 rather than a direct effect of amyloid deposition. Longitudinal studies are however needed to explore the causal relationship between APOE status, amyloid, and perfusion. In this sense, future amyloid PET studies will be useful to clarify the topographical relations between amyloid deposition and brain perfusion.

LIN perfusion was also associated with episodic memory impairment, in line with LIN topography and function, since the medial temporal lobe is critically involved in episodic memory [27,28] Previous studies reported an association between the episodic memory decline and hypoperfusion in the DMN areas (i.e. middle frontal cortex [33] and anterior cingulate cortex [33,40]). Our finding of an association with APOE ε4, amyloid and worse memory performance (i.e., increasing number of errors), but not with tau or neurodegeneration, suggests that LIN hypoperfusion might be related to cognitive deficits through APOE or Aβ-related processes rather than tau- or neurodegeneration-related processes. Indeed, in our sample the episodic memory impairment showed a correlation with $A\beta_{42}$ and differed between ε4+ and ε4-, supporting our hypothesis of a downstream role of APOE in influencing Aβ-mediated processes in AD cognitive features. The present results could however be related to the fact that the PAL is a spatial memory task and recent findings using PET amyloid ligands reported a relation between a spatial hippocampus dependent memory task and the presence of amyloid [65]. Taken together, these results suggest that, at least in this sample, amyloidosis but not tau plays a role in the association between spatial memory and limbic hypoperfusion.

When focusing on vascular damage, we did not find any association between WMHs and CBF in any NOIs. A possible explanation may be that vascular damage is primarily associated to tau pathology and neurodegeneration [66,67], and, therefore, the association with vascular and neurodegenerative features may occur later in AD course.

The discriminant validity was largely supported by our results, as no association emerged between DMN and/or LIN perfusion and the selected AD-unrelated features. Similarly, no association was detected between CBF in AD unrelated networks and AD features.

The major strength of this study is the comprehensive assessment of perfusion in relation with AD pathophysiological features, and the use of a network-based approach. Indeed, it has been previously reported that amyloid and tau proteins spread through functionally connected areas [68,69]. Focusing on brain networks rather than on single regions would better reflect the underling pathology. This study also has several limitations. First, the small sample size limits the generalizability of the results and some associations did not survive multiple comparison correction. Thus, our results should be taken with caution and further studies in larger samples are needed to confirm our results. A second limitation is that some parameters of our ASL sequence are sub-optimal in the current state-of-the-art and other protocols such as pseudocontinuous ASL with 3D acquisition are generally recommended for studies in neurodegenerative diseases [49]. Moreover, as the elderly population is generally affected by occlusion and / or stenosis of large vessel, future studies should consider the usage of more advanced sequences, such as multi-TI or velocity-selective ASL, to limit the effect of delayed arterial transit time. However, despite these sequence limitations, we found significant results which seem to be very promising for future ASL application in the AD clinical setting. Another limitation is the use of CSF instead of PET to measure Aβ and tau levels, which did not enable us to investigate local/regional

effects. However, a possible advantage of CSF is that it may detect amyloid alterations earlier than PET due to better technical sensitivity [70]. Finally, there is a temporal mismatch between CSF assessment and ASL MRI acquisition, as the first was conducted after 18 months and the latter after 24 months. Future studies including MRI and CSF data collected at similar timepoints will be important to confirm our results.

CONCLUSION

Our results support the validity of DMN and LIN perfusion as AD markers in aMCI, indicating a significant association between CBF and amyloidosis, APOE ε4, and memory impairment.

ACKNOWLEDGMENTS

PharmaCog is funded by the EU-FP7 for the Innovative Medicine Initiative (grant no. 115009). We wish to thank all the co-Investigators from our Study Group (WP5-PharmaCog/European Alzheimer's Disease Neuroimaging Initiative) (for the complete list see Supplementary Table 3). Moreover, we are grateful to all members and collaborators of the PharmaCog project, and particularly to Luigi Antelmi and Daniele Orlandi.

CONFLICT OF INTEREST/DISCLOSURE STATEMENT

The authors have no conflict of interest to report.

REFERENCE LIST

[1] Petersen RC (2009) Early diagnosis of Alzheimer's disease: is MCI too late? *Curr Alzheimer Res* **6**, 324-30.

[2] Prestia A, Caroli A, van der Flier WM, Ossenkoppele R, Van Berckel B, Barkhof F, Teunissen CE, Wall AE, Carter SF, Scholl M, Choo IH, Nordberg A, Scheltens P, Frisoni GB (2013) Prediction of dementia in MCI patients based on core diagnostic markers for Alzheimer disease. *Neurology* **80**, 1048-1056.

[3] Mattsson N, Zetterberg H, Hansson O, Andreasen N, Parnetti L, Jonsson M, Herukka S, van der Flier WM, Blankenstein MA, Ewers M, Rich K, Kaiser E, Verbeek M, Tsolaki M, Mulugeta E, Rosén E, Aarsland D, Visser PJ, Schröder J, Marcusson J, de Leon M, Hampel H, Scheltens P, Pirttilä T, Wallin A, Jönhagen ME, Minthon L, Winblad B, Blennow K (2009) CSF biomarkers and incipient Alzheimer disease in patients with mild cognitive impairment. *JAMA* **302**, 385-393.

[4] Jack Jr CR, Knopman DS, Jagust WJ, Shaw LM, Aisen PS, Weiner MW, Petersen RC, Trojanowski JQ (2010) Hypothetical model of dynamic biomarkers of the Alzheimer's pathological cascade. *Lancet Neurol* **9**, 119-128.

[5] Sperling RA, Aisen PS, Beckett LA, Bennett DA, Craft S, Fagan AM, Iwatsubo T, Jack Jr CR, Kaye J, Montine TJ, Park DC, Reiman EM, Rowe CC, Siemers E, Stern Y, Yaffe K, Carrillo MC, Thies B, Morrison-Bogorad M, Wagster MV, Phelps CH (2011) Toward defining the preclinical stages of Alzheimer's disease: Recommendations from the National Institute on Aging-Alzheimer's Association workgroups on diagnostic guidelines for Alzheimer's disease. *Alzheimers Dement* **7**, 280-292.

[6] Kisler K, Nelson AR, Montagne A, Zlokovic BV (2017) Cerebral blood flow regulation and neurovascular dysfunction in Alzheimer disease. *Nat Rev Neurosci* **18**, 419-434.

[7] Jezzard P, Chappell MA, Okell TW (2018) Arterial spin labeling for the measurement of cerebral perfusion and angiography. *J Cereb Blood Flow Metab* **38**, 603-626.

[8] Williams DS, Detre JA, Leigh JS, Koretsky AP (1992) Magnetic resonance imaging of perfusion using spin inversion of arterial water. *Proc Natl Acad Sci U S A* **89**, 212-216.

[9] Zhang N, Gordon ML, Goldberg TE (2017) Cerebral blood flow measured by arterial spin labeling MRI at resting state in normal aging and Alzheimer's disease. *Neurosci Biobehav Rev* **72**, 168-175.

[10] Bangen KJ, Restom K, Liu TT, Wierenga CE, Jak AJ, Salmon DP, Bondi MW (2012) Assessment of Alzheimer's disease risk with functional magnetic resonance imaging: an arterial spin labeling study. *J Alzheimer's Dis* **31**, S59-S74.

[11] Lou W, Shi L, Wong A, Chu WC, Mok VC, Wang D (2016) Changes of cerebral perfusion and functional brain network organization in patients with mild cognitive impairment. *J Alzheimer's Dis* **54**, 397-409.

[12] Johnson NA, Jahng G, Weiner MW, Miller BL, Chui HC, Jagust WJ, Gorno-Tempini ML, Schuff N (2005) Pattern of cerebral hypoperfusion in Alzheimer disease and mild cognitive impairment measured with arterial spin-labeling MR imaging: initial experience. *Radiology* **234**, 851-859.

[13] Alexopoulos P, Sorg C, Förschler A, Grimmer T, Skokou M, Wohlschläger A, Perneczky R, Zimmer C, Kurz A, Preibisch C (2012) Perfusion abnormalities in mild cognitive impairment and mild

dementia in Alzheimer's disease measured by pulsed arterial spin labeling MRI. *Eur Arch Psychiatry Clin Neurosci* **262**, 69-77.

[14] Okonkwo OC, Xu G, Oh JM, Dowling NM, Carlsson CM, Gallagher CL, Birdsill AC, Palotti M, Wharton W, Hermann BP, LaRue A, Bendlin BB, Rowley HA, Asthana S, Sager MA, Johnson SC (2014) Cerebral blood flow is diminished in asymptomatic middle-aged adults with maternal history of Alzheimer's disease. *Cereb Cortex* **24**, 978-988.

[15] Michels L, Warnock G, Buck A, Macauda G, Leh SE, Kaelin AM, Riese F, Meyer R, O'Gorman R, Hock C, Kollias S, Gietl AF (2016) Arterial spin labeling imaging reveals widespread and Aβ-independent reductions in cerebral blood flow in elderly apolipoprotein epsilon-4 carriers. *J Cereb Blood Flow Metab* **36**, 581-595.

[16] Kim C, Alvarado RL, Stephens K, Wey H, Wang DJJ, Leritz EC, Salat DH (2020) Associations between cerebral blood flow and structural and functional brain imaging measures in individuals with neuropsychologically defined mild cognitive impairment. *Neurobiol Aging* **86**, 64-74.

[17] Pievani M, Filippini N, Van Den Heuvel, Martijn P, Cappa SF, Frisoni GB (2014) Brain connectivity in neurodegenerative diseases—from phenotype to proteinopathy. *Nat Revs Neurol* **10**, 620-633.

[18] Badhwar A, Tam A, Dansereau C, Orban P, Hoffstaedter F, Bellec P (2017) Resting-state network dysfunction in Alzheimer's disease: a systematic review and meta-analysis. *Alzheimers Demen* (Amst) **8**, 73-85.

[19] Pini L, Geroldi C, Galluzzi S, Baruzzi R, Bertocchi M, Chitò E, Orini S, Romano M, Cotelli M, Rosini S, Magnaldi S, Morassi M, Cobelli M, Bonvicini C, Archetti S, Zanetti O, Frisoni GB, Pievani

M (2020) Age at onset reveals different functional connectivity abnormalities in prodromal Alzheimer's disease. *Brain Imaging Behav* **14**, 2594-2605.

[20] De Vogelaere F, Santens P, Achten E, Boon P, Vingerhoets G (2012) Altered default-mode network activation in mild cognitive impairment compared with healthy aging. *Neuroradiology* **54**, 1195-1206.

[21] Lee E, Yoo K, Lee Y, Chung J, Lim J, Yoon B, Jeong Y (2016) Default mode network functional connectivity in early and late mild cognitive impairment. *Alzheimer Dis Assoc Disord* **30**, 289-296.

[22] Gour N, Felician O, Didic M, Koric L, Gueriot C, Chanoine V, Confort-Gouny S, Guye M, Ceccaldi M, Ranjeva JP (2014) Functional connectivity changes differ in early and late-onset alzheimer's disease. *Hum Brain Mapp* **35**, 2978-2994.

[23] Maass A, Berron D, Harrison TM, Adams JN, La Joie R, Baker S, Mellinger T, Bell RK, Swinnerton K, Inglis B, Rabinovici GD, Düzel E, Jagust WJ (2019) Alzheimer's pathology targets distinct memory networks in the ageing brain. *Brain* **142**, 2492-2509.

[24] Braak H, Braak E (1997) Frequency of stages of Alzheimer-related lesions in different age categories. *Neurobiol Aging* **18**, 351-357.

[25] Palmqvist S, Schöll M, Strandberg O, Mattsson N, Stomrud E, Zetterberg H, Blennow K, Landau S, Jagust W, Hansson O (2017) Earliest accumulation of β-amyloid occurs within the default-mode network and concurrently affects brain connectivity. *Nat Commun* **8**, 1-13.

[26] Cho H, Lee HS, Choi JY, Lee JH, Ryu YH, Lee MS, Lyoo CH (2018) Predicted sequence of cortical tau and amyloid-β deposition in Alzheimer disease spectrum. *Neurobiol Aging* **68**, 76-84.

[27] Ranganath C, Ritchey M (2012) Two cortical systems for memory-guided behaviour. *Nat Rev Neurosc* **13**, 713-726.

[28] Catani M, Dell'Acqua F, De Schotten MT (2013) A revised limbic system model for memory, emotion and behaviour. *Neurosci Biobehav Rev* **37**, 1724-1737.

[29] Barbeau E, Didic M, Tramoni E, Felician O, Joubert S, Sontheimer A, Ceccaldi M, Poncet M (2004) Evaluation of visual recognition memory in MCI patients. *Neurology* **62**, 1317-1322.

[30] Tosun D, Schuff N, Rabinovici GD, Ayakta N, Miller BL, Jagust W, Kramer J, Weiner MM, Rosen HJ (2016) Diagnostic utility of ASL-MRI and FDG-PET in the behavioral variant of FTD and AD. *Ann Clinical Transll Neurol* **3**, 740-751.

[31] Hays CC, Zlatar ZZ, Wierenga CE (2016) The utility of cerebral blood flow as a biomarker of preclinical Alzheimer's disease. *Cell Mol Neurobiol* **36**, 167-179.

[32] Binnewijzend MA, Kuijer JP, Benedictus MR, van der Flier, Wiesje M, Wink AM, Wattjes MP, van Berckel BN, Scheltens P, Barkhof F (2013) Cerebral blood flow measured with 3D pseudocontinuous arterial spin-labeling MR imaging in Alzheimer disease and mild cognitive impairment: a marker for disease severity. *Radiology* **267**, 221-230.

[33] Chao LL, Buckley ST, Kornak J, Schuff N, Madison C, Yaffe K, Miller BL, Kramer JH, Weiner MW (2010) ASL perfusion MRI predicts cognitive decline and conversion from MCI to dementia. *Alzheimer Dis Assoc Disord* **24**, 19-27.

[34] Mattsson N, Tosun D, Insel PS, Simonson A, Jack Jr CR, Beckett LA, Donohue M, Jagust W, Schuff N, Weiner MW (2014) Association of brain amyloid-β with cerebral perfusion and structure in Alzheimer's disease and mild cognitive impairment. *Brain* **137**, 1550-1561.

[35] Kikukawa T, Abe T, Ataka S, Saito H, Hasegawa I, Mino T, Takeuchi J, Kawabe J, Wada Y, Watanabe Y, Itoh Y (2018) Amyloid deposition and CBF patterns predict conversion of mild cognitive impairment to dementia. *Neurol Sci* **39**, 1597-1602.

[36] Tosun D, Schuff N, Jagust W, Weiner MW, Alzheimer"s Disease Neuroimaging Initiative (2016) Discriminative Power of Arterial Spin Labeling Magnetic Resonance Imaging and 18F-Fluorodeoxyglucose Positron Emission Tomography Changes for Amyloid-beta-Positive Subjects in the Alzheimer's Disease Continuum. *Neurodegener Dis* **16**, 87-94.

[37] Habert M, de Souza LC, Lamari F, Daragon N, Desarnaud S, Jardel C, Dubois B, Sarazin M (2010) Brain perfusion SPECT correlates with CSF biomarkers in Alzheimer's disease. *Eur J Nucl Med Mol Imaging* **37**, 589-593.

[38] Leuzy A, Rodriguez-Vieitez E, Saint-Aubert L, Chiotis K, Almkvist O, Savitcheva I, Jonasson M, Lubberink M, Wall A, Antoni G, Nordberg A (2018) Longitudinal uncoupling of cerebral perfusion, glucose metabolism, and tau deposition in Alzheimer's disease. *Alzheimers Dement* **14**, 652-663.

[39] Caroli A, Testa C, Geroldi C, Nobili F, Guerra UP, Bonetti M, Frisoni GB (2007) Brain perfusion correlates of medial temporal lobe atrophy and white matter hyperintensities in mild cognitive impairment. *J Neurol* **254**, 1000-1008.

[40] De Vis JB, Peng S, Chen X, Li Y, Liu P, Sur S, Rodrigue KM, Park DC, Lu H (2018) Arterial-spin-labeling (ASL) perfusion MRI predicts cognitive function in elderly individuals: A 4-year longitudinal study. *J Magn Reson Imaging* **48**, 449-458.

[41] Wierenga CE, Dev SI, Shin DD, Clark LR, Bangen KJ, Jak AJ, Rissman RA, Liu TT, Salmon DP, Bondi MW (2012) Effect of mild cognitive impairment and APOE genotype on resting cerebral blood flow and its association with cognition. *J Cerebl Blood Flow Metab* **32**, 1589-1599.

[42] Kim SM, Kim MJ, Rhee HY, Ryu C, Kim EJ, Petersen ET, Jahng G (2013) Regional cerebral perfusion in patients with Alzheimer's disease and mild cognitive impairment: effect of APOE epsilon4 allele. *Neuroradiology* **55**, 25-34.

[43] Chhatwal JP, Schultz AP, Johnson KA, Hedden T, Jaimes S, Benzinger TL, Jack Jr C, Ances BM, Ringman JM, Marcus DS, Ghetti B, Farlow MR, Danek A, Levin J, Yakushev I, Laske C, Koeppe RA, Galasko DR, Xiong C, Masters CL, Schofield PR, Kinnunen KM, Salloway S, Martins RN, McDade E, Cairns NJ, Buckles VD, Morris JC, Bateman R, Sperling RA (2018) Preferential degradation of cognitive networks differentiates Alzheimer's disease from ageing. *Brain* **141**, 1486-1500.

[44] Grothe MJ, Teipel SJ, Alzheimer's Disease Neuroimaging Initiative (2016) Spatial patterns of atrophy, hypometabolism, and amyloid deposition in Alzheimer's disease correspond to dissociable functional brain networks. *Hum Brain Mapp* **37**, 35-53.

[45] Firth NC, Primativo S, Brotherhood E, Young AL, Yong KX, Crutch SJ, Alexander DC, Oxtoby NP (2020) Sequences of cognitive decline in typical Alzheimer's disease and posterior cortical atrophy estimated using a novel event-based model of disease progression. *Alzheimers Dement* **16**, 965-973.

[46] Galluzzi S, Marizzoni M, Babiloni C, Albani D, Antelmi L, Bagnoli C, Bartres-Faz D, Cordone S, Didic M, Farotti L, Fiedler U, Forloni G, Girtler N, Hensch T, Jovicich J, Leeuwis A, Marra C, Molinuevo JL, Nobili F, Pariente J, Parnetti L, Payoux P, Del Percio C, Ranjeva JP, Rolandi E, Rossini PM, Schönknecht P, Soricelli A, Tsolaki M, Visser PJ, Wiltfang J, Richardson JC, Bordet R, Blin O, Frisoni GB (2016) Clinical and biomarker profiling of prodromal Alzheimer's disease in workpackage 5 of the Innovative Medicines Initiative PharmaCog project: a 'European ADNI study'. *J Intern Med* **279**, 576-591.

[47] Jovicich J, Marizzoni M, Sala-Llonch R, Bosch B, Bartrés-Faz D, Arnold K, Benninghoff J, Wiltfang J, Roccatagliata L, Nobili F, Hensch T, Tränkner A, Schönknecht P, Leroy M, Lopes R, Bordet R, Chanoine V, Ranjeva JP, Didic M, Gros-Dagnac H, Payoux P, Zoccatelli G, Alessandrini F, Beltramello A, Bargalló N, Blin O, Frisoni Gb (2013) Brain morphometry reproducibility in multi-center 3T MRI studies: a comparison of cross-sectional and longitudinal segmentations. *Neuroimage* **83**, 472-84.

[48] Buxton RB, Frank LR, Wong EC, Siewert B, Warach S, Edelman RR (1998) A general kinetic model for quantitative perfusion imaging with arterial spin labeling. *Magn Reson Med* **40**, 383-396.

[49] Alsop DC, Detre JA, Golay X, Günther M, Hendrikse J, Hernandez-Garcia L, Lu H, MacIntosh BJ, Parkes LM, Smits M, van Osch MJP, Wang DJJ, Wong EC, Zaharchuk G (2015) Recommended implementation of arterial spin-labeled perfusion MRI for clinical applications: a consensus of the ISMRM perfusion study group and the European consortium for ASL in dementia. *Magn Reson Med* **73**, 102-116.

[50] Du AT, Jahng GH, Hayasaka S, Kramer JH, Rosen HJ, Gorno-Tempini ML, Rankin KP, Miller BL, Weiner MW, Schuff N (2006) Hypoperfusion in frontotemporal dementia and Alzheimer disease by arterial spin labeling MRI. *Neurology* **67**, 1215-1220.

[51] Schaefer A, Kong R, Gordon EM, Laumann TO, Zuo X, Holmes AJ, Eickhoff SB, Yeo BT (2018) Local-global parcellation of the human cerebral cortex from intrinsic functional connectivity MRI. *Cereb Cortex* **28**, 3095-3114.

[52] Backhausen LL, Herting MM, Buse J, Roessner V, Smolka MN, Vetter NC (2016) Quality control of structural MRI images applied using FreeSurfer—a hands-on workflow to rate motion artifacts. *Front Neurosci* **10**, 558.

[53] Dale AM, Fischl B, Sereno MI (1999) Cortical surface-based analysis: I. Segmentation and surface reconstruction. *Neuroimage* **9**, 179-194.

[54] Fischl B, Sereno MI, Dale AM (1999) Cortical surface-based analysis: II: inflation, flattening, and a surface-based coordinate system. *Neuroimage* **9**, 195-207.

[55] Fischl B, Salat DH, Busa E, Albert M, Dieterich M, Haselgrove C, Van Der Kouwe A, Killiany R, Kennedy D, Klaveness S, Montillo A, Makris N, Rosen B, Dale AM (2002) Whole brain segmentation: automated labeling of neuroanatomical structures in the human brain. *Neuron* **33**, 341-355.

[56] Schmidt P, Gaser C, Arsic M, Buck D, Förschler A, Berthele A, Hoshi M, Ilg R, Schmid VJ, Zimmer C, Hemmer B, Mühlau M (2012) An automated tool for detection of FLAIR-hyperintense white-matter lesions in multiple sclerosis. *Neuroimage* **59**, 3774-3783.

[57] Ribaldi F, Altomare D, Jovicich J, Ferrari C, Picco A, Pizzini FB, Soricelli A, Mega A, Ferretti A, Drevelegas A, Bosch B, Müller BW, Marra C, Cavaliere C, Bartrés-Faz D, Nobili F, Alessandrini F, Barkhof F, Gros-Dagnac H, Ranjeva JP, Wiltfang J, Kuijer J, Sein J , Hoffmann KT, Roccatagliata L, Parnetti P, Tsolaki M, Constantinidis M, Aiello M, Salvatore M, Montalti M, Caulo M, Didic M, Bargallo N, Blin O, Rossini PM, Schonknecht P, Floridi P, Payoux P, Visser PJ, Bordet R, Lopes R, Tarducci R, Bombois S, Hensch T, Fiedler U, Richardson JC, Frisoni GB, Marizzoni M (2020) Accuracy and reproducibility of automated white matter hyperintensities segmentation with lesion segmentation tool: A European multi-site 3T study. *Magn Reson Imaging* **76**, 108-115.

[58] Mattsson N, Andreasson U, Persson S, Arai H, Batish SD, Bernardini S, Bocchio-Chiavetto L, Blankenstein MA, Carrillo MC, Chalbot S, Coart E, Chiasserini D, Cutler N, Dahlfors G, Duller S, Fagan AM, Forlenza O, Frisoni GB, Galasko D, Galimberti D, Hampel H, Handberg A, Heneka MT, Herskovits AZ, Herukka SK, Holtzman DM, Humpel C, Hyman BT, Iqbal K, Jucker M, Kaeser SA, Kaiser E, Kapaki E, Kidd D, Klivenyi P, Knudsen CS, Kummer MP, Lui, J Lladó A, Lewczuk P, Li QX, Martins R, Masters C, McAuliffe J, Mercken M, Moghekar A, Molinuevo JL, J Montine TJ, Nowatzke W, O'Brien R, Otto M, Paraskevas GP, Parnetti L, Petersen RC, Prvulovic D, de Reus HPM, Rissman RA, Scarpini E, Stefani A, Soininen H, Schröder J, Shaw LM, Skinningsrud A, Skrogstad B, Spreer A, Talib L, Teunissen C, Trojanowski JQ, Tumani H, Umek RM, Van Broeck B, Vanderstichele H, Vecsei L, Verbeek MM, Windisch M, Zhang J, Zetterberg H, Blennow K (2011) The Alzheimer's Association external quality control program for cerebrospinal fluid biomarkers. *Alzheimers Dement* **7**, 386-395. e6.

[59] Nathan PJ, Lim YY, Abbott R, Galluzzi S, Marizzoni M, Babiloni C, Albani D, Bartres-Faz D, Didic M, Farotti L, Parnetti L, Salvadori N, Müller BW, Forloni G, Girtler N, Hensch T, Jovicich J,

Leeuwis A, Marra C, Molinuevo JL, Nobili F, Pariente J, Payoux P, Ranjeva JP, Rolandi E, Rossini PM, Schönknecht P, Soricelli A, Tsolaki M, Visser PJ, Wiltfang J, Richardson JC, Bordet R, Blin O, Frisoni GB (2017) Association between CSF biomarkers, hippocampal volume and cognitive function in patients with amnestic mild cognitive impairment (MCI). *Neurobiol Aging* **53**, 1-10.

[60] Marizzoni M, Ferrari C, Babiloni C, Albani D, Barkhof F, Cavaliere L, Didic M, Forloni G, Fusco F, Galluzzi S, Hensch T, Jovicich J, Marra C, Molinuevo JL, Nobili F, Parnetti L, Payoux P, Ranjeva JL, Ribaldi F, Rolandi E, Rossini PM, Salvatore M, Soricelli A, Tsolaki M, Visser PJ, Wiltfang J, Richardson JC, Bordet R, Blin O, Frisoni GB (2019) CSF cut-offs for MCI due to AD depend on APOEε4 carrier status. *Neurobiol Aging* **89**, 55-62.

[61] Luckhaus C, Cohnen M, Flüß MO, Jänner M, Grass-Kapanke B, Teipel SJ, Grothe M, Hampel H, Peters O, Kornhuber J, Maier W, Supprian T, Gaebel W, Mödder U, Wittsack HJ (2010) The relation of regional cerebral perfusion and atrophy in mild cognitive impairment (MCI) and early Alzheimer's dementia. *Psychiatry Res* **183**, 44-51.

[62] Liu J, Zhang X, Yu C, Duan Y, Zhuo J, Cui Y, Liu B, Li K, Jiang T, Liu Y (2016) Impaired parahippocampus connectivity in mild cognitive impairment and Alzheimer's disease. *J Alzheimers Dis* **49**, 1051-1064.

[63] Halliday MR, Rege SV, Ma Q, Zhao Z, Miller CA, Winkler EA, Zlokovic BV (2016) Accelerated pericyte degeneration and blood–brain barrier breakdown in apolipoprotein E4 carriers with Alzheimer's disease. *J Cereb Blood Flow Metab* **36**, 216-227.

[64] Liu C, Kanekiyo T, Xu H, Bu G (2013) Apolipoprotein E and Alzheimer disease: risk, mechanisms and therapy. *Nat Rev Neuro* **9**, 106-108.

[65] Webb CE, Foster CM, Horn MM, Kennedy KM, Rodrigue KM (2020) Beta-amyloid burden predicts poorer mnemonic discrimination in cognitively normal older adults. *Neuroimage* **221**, 117199.

[66] Tosto G, Zimmerman ME, Hamilton JL, Carmichael OT, Brickman AM, Alzheimer's Disease Neuroimaging Initiative (2015) The effect of white matter hyperintensities on neurodegeneration in mild cognitive impairment. *Alzheimers Dement* **11**, 1510-1519.

[67] McAleese KE, Firbank M, Dey M, Colloby SJ, Walker L, Johnson M, Beverley JR, Taylor JP, Thomas AJ, O'Brien JT, Attems J (2015) Cortical tau load is associated with white matter hyperintensities. *Acta Neuropathol Commun* **3**, 1-11.

[68] Pereira JB, Ossenkoppele R, Palmqvist S, Strandberg TO, Smith R, Westman E, Hansson O (2019) Amyloid and tau accumulate across distinct spatial networks and are differentially associated with brain connectivity. *Elife* **8**, e50830.

[69] Vogel JW, Iturria-Medina Y, Strandberg OT, Smith R, Levitis E, Evans AC, Hansson O (2020) Spread of pathological tau proteins through communicating neurons in human Alzheimer's disease. *Nat Commun* **11**, 1-15.

[70] Palmqvist S, Mattsson N, Hansson O, Alzheimer's Disease Neuroimaging Initiative (2016) Cerebrospinal fluid analysis detects cerebral amyloid-β accumulation earlier than positron emission tomography. *Brain* **139**, 1226-1236.

Table 1. Demographic, clinical, biomarker, and genetic features of MCI patients.

Demographic characteristics	**MCI (N = 14)** **mean (SD) [range]**
Age, years	72.8 (7.2) [63.0 – 86.0]
Education, years	11.7 (5.2) [3.0 – 18.0]
Female sex, n (%)	5 (36%)
Cognition, function, mood and behavior	
Mini-mental state examination	26.1 (1.8) [23.0 – 29.0]
Alzheimer's Disease Assessment Scale	23.5 (6.8) [12.7 – 41.7]
Functional assessment questionnaire	5.9 (5.1) [0.0 – 18.0]
Geriatric depression scale	4.8 (4.9) [0.0 – 16.0]
CSF protein level, pg/ml (min-max)	
Aβ42	647 (258) [314 - 1075] [a]
P-tau	71 (27) [32 – 124] [a]
T-tau	581 (252) [191 – 1081] [a]
Aβ42/p-tau ratio, positive (%) [50]	7 (58%) [a]
Genetic	
APOE ε4 carriers, n (%)	8 (57%)

[a] Data missing for 2 patients

Abbreviations: MCI, mild cognitive impairment; CSF, cerebrospinal fluid; $A\beta_{42}$, amyloid β peptide 1-42; t-tau, total tau protein; p-tau, phospho-tau protein; APOE, the Apolipoprotein E gene; ε4, allele 4 of the Apolipoprotein E gene; pg/ml, picogram/milliliter.

Table 2. Brain perfusion**,** neurodegenerative, cognitive, and vascular features of MCI patients. Volumes are corrected for total intracranial volume.

Brain perfusion (ml/100g/min)	**Mean (SD) [range]**
Default mode network	26.3 (4.0) [21.8 – 34.8]
Limbic network	29.5 (4.8) [21.3 – 39.4]
Somatomotor network	26.8 (5.2) [20.7 – 40.0]
Visual network	27.4 (4.0) [22.0 – 36.3]
Neurodegeneration markers	
Hippocampal volume, cm^3	3.2 (0.4) [2.5 -3.9]
Cerebellar cortex, cm^3	46 (9) [26 – 56]
Cognitive features	
Episodic memory	
Paired associate learning test, number of errors[b]	86 (33) [32 – 142]
Processing speed	
Five-choice reaction time, ms[b]	400 (65) [309 – 540]
Vascular burden	
White matter lesion volume, cm^3	3.32(7.02) [0-26.11]

[b] Test from the Cambridge Neuropsychological Test Automated Battery (CANTAB).

Abbreviations: SD, standard deviation; ml, milliliters; g, grams; min, minutes; mm, millimeters; cm, centimeters; ms, milliseconds.

SUPPLEMENTARY MATERIAL

Supplementary Table 1. Summary of MRI features and protocols across MRI sites.

	Site 1	**Site 2**	**Site 3**
MRI site location	Verona [a]	Marseille	Naples
MRI scanner	Siemens Allegra	Siemens Verio	Siemens Biograph mMR
MRI system software version	VA25A	B17	B18P
TX / RX coil	Birdcage	Body/12-channels	Body/12-channels
Parallel imaging: method, acceleration	None	GRAPPA 2	GRAPPA 2
3D T1 acquisition			
TE (ms, shortest)	2.83	2.98	2.96
TR (ms)	2300	2300	2300
Voxel size (mm^3)	1x1x1	1x1x1	1x1x1
Flip angle (degrees)	9	9	9
Slices (n)	176	178	176
Slice orientation	Sagittal	Sagittal	Sagittal
FoV (mm)	256	256	256
Acquisition time (min:sec)	09:50	05:12	05:03
2D FLAIR acquisition			
TE (ms)	86	90	90
TR (ms)	9760	9000	9000
Voxel size (mm^3)	0.9x0.9x4	0.9x0.9x4	0.9x0.9x4
Slices (n)	44	44	44
Slice orientation	Axial	Axial	axial
FoV	230	230	230
Acquisition matrix	256 x 256	256 x 256	256 x 256

Acquisition time (min:sec)	09:18	04:59	3:43
2D ASL acquisition			
TE (ms, shortest)	16	17	17
TR (ms)	3500	3500	3500
Labeling Type	Pulsed PICORE Q2TIPS	Pulsed PICORE Q2TIPS	Pulsed PICORE Q2TIPS
Inversion Times TI1/T1s/TI2 (ms)	800/1500/2000	800/1500/2000	800/1500/2000
Measurements (n)	120	120	120
Voxel size (mm^3)	3.5x3.5x5	3.5x3.5x5	3.5x3.5x4.5
Flip angle (degrees)	90	90	90
Slices (n)	26	26	26
Slice orientation	Axial	Axial	Axial
FOV	226	242	224
Acquisition time (min:sec)	07:12	~ 07:00	07:09

[a] MRI acquisitions for subjects enrolled in Brescia.

Supplementary Table 2. Neuropsychological assessment of MCI patients.

Verbal memory	**Mean (SD) [range]**
RAVLT, immediate recall	27.1 (6.7) [14 – 37]
RAVLT, delayed recall	1.9 (3.4) [0 – 12]
Visual memory	
Paired associate learning test (number of errors) [a]	86.3 (33.1) [32.0 – 142.0]
Delayed matching to sample (% correct all delays) [a]	64.9 (15.1) [46.7 – 87.5]
Spatial recognition memory test (% correct) [a]	61.8 (13.1) [35.0 – 80.0]
Pattern recognition memory test (% correct) [a]:	
Immediate	78.6 (14.1) [50.0 – 100.0]
Delayed	72.0 (10.1) [50.0 – 92.0]
Working memory	
Digit span forward	5.0 (1.0) [3.0 – 6.0]
Digit span backward	3.6 (0.9) [2.0 – 5.0]
Spatial working memory test (number of errors) [a]	37.2 (17.0) [22.0 – 71.0]
Attention and processing speed	
Trial making test A (s)	54 (30) [30 – 150]
Processing speed [a]	
Five-choice reaction time (ms)	400 (65) [309 – 540]
Five-choice movement time (ms)	517 (210) [355 – 1054]
Rapid visual information processing [b]	0.8 (0.0) [0.75 – 0.88]
Language	
Letter fluency	28.5 (12.7) [9.0 – 45.0]
Category fluency	28.9 (11.6) [8.0 – 49.0]

Boston Naming Test	19.1 (6.4) [5.0 – 28.0]
Executive functions and planning abilities	
Trial making test B (s)	183 (87) [60 – 300]
Clock drawing test	4.2 (1.1) [1.0 – 5.0]

[a] Test from the Cambridge Neuropsychological Test Automated Battery (CANTAB).

[b] Data missing for 3 patients

Abbreviations: MCI, mild cognitive impairment; RAVL, Rey Auditory Verbal Learning Test; SD, standard deviation; s, seconds; ms, milliseconds.

Supplementary Table 3. PharmaCog - WP5/European ADNI Acknowledgement List.

Name	Affiliation	Role in the project
Giovanni B Frisoni	University Hospitals and University of Geneva, Geneva, Switzerland; IRCCS Istituto Centro San Giovanni di Dio Fatebenefratelli, Brescia, Italy	WP5 PI
Oliver Blin	Aix Marseille University, Marseille, France	WP5 CoPI
Samantha Galluzzi	IRCCS Istituto Centro San Giovanni di Dio Fatebenefratelli, Brescia, Italy	WP5 Clinical core leader
Valeria Drago	IRCCS Istituto Centro San Giovanni di Dio Fatebenefratelli, Brescia, Italy	WP5 Clinical core co-leader
Jorge Jovicich	Center for Mind/Brain Sciences, University of Trento, Italy	WP5 MRI core leader
Moira Marizzoni	IRCCS Istituto Centro San Giovanni di Dio Fatebenefratelli, Brescia, Italy	WP5 MRI core co-leader
Gianluigi Forloni	Istituto di Ricerche Farmacologiche Mario Negri IRCCS, Milano, Italy	WP5 Biological core leader
Diego Albani	Istituto di Ricerche Farmacologiche Mario Negri IRCCS, Milano, Italy	WP5 Biological core co-leader
Claudio Babiloni	Department of Physiology and Pharmacology "V. Erspamer", Sapienza University of Rome, Rome, Italy; IRCCS San Raffaele Pisana of Rome and Cassino, Rome and Cassino, Italy	WP5 EEG core leader
Alberto Redolfi	IRCCS Istituto Centro San Giovanni di Dio Fatebenefratelli, Brescia, Italy	WP5 Bioinformatic core leader
Libera Cavaliere	IRCCS Istituto Centro San Giovanni di Dio Fatebenefratelli, Brescia, Italy	WP5 Project manager
Cristina Bagnoli	IRCCS Istituto Centro San Giovanni di Dio Fatebenefratelli, Brescia, Italy	WP5 Project manager
Chiara Barattieri	IRCCS Istituto Centro San Giovanni di Dio Fatebenefratelli, Brescia, Italy	WP5 Project manager
Severine Pitel	Qualissima, Marseille, France	WP5 Project manager
Romain Combalat	Qualissima, Marseille, France	WP5 Project manager
Jill Richardson	Neurosciences Therapeutic Area, GlaxoSmithKline R&D, Gunnels Wood Road, Stevenage, United Kingdom	PharmaCog Project Coordinator
Regis Bordet	University of Lille, Inserm, CHU Lille, U1171 - Degenerative and vascular cognitive disorders, F-59000 Lille, France	PharmaCog Academic Coordinator

By site

WP5 Site	Name	Role in the project
Amsterdam	Pieter Jelle Visser	Site PI
Amsterdam	Frederik Barkhof	Site Investigator
Amsterdam	Joost Kuijer	Site Investigator
Amsterdam	Annebet Leeuwis	Site Investigator
Barcelona	José Luis Molinuevo	Site PI
Barcelona	David Bartrés-Faz	Site PI
Barcelona	Juan Pablo Martín-Trias	Site Investigator
Barcelona	Lorena Rami	Site Investigator
Barcelona	Beatriz Bosch	Site Investigator
Brescia	Giovanni B Frisoni	Site PI
Brescia	Samantha Galluzzi	Site Investigator
Brescia	Alberto Beltramello	Site Investigator
Brescia	Giada Zoccatelli	Site Investigator
Brescia	Luisella Bocchio Chiavetto	Site Investigator
Brescia	Elisabetta Maffioletti	Site Investigator
Brescia	Davide Moretti	Site Investigator
Brescia	Maura Parapini	Site Investigator
Brescia	Maria Cotelli	Site Investigator
Brescia	Melissa Romano	Site Investigator

Brescia	Luca Venturi	Site Investigator
Brescia	Luigi Antelmi	Site Investigator
Brescia	Daniele Tolomeo	Site Investigator
Brescia	Genoveffa Borsci	Site Investigator
Essen	Jens Wiltfang	Site PI
Essen	BW Müller	Site Investigator
Genoa	Flavio Nobili	Site PI
Genoa	Agnese Picco	Site Investigator
Genoa	Nicola Girtler	Site Investigator
Genoa	Luca Roccatagliata	Site Investigator
Genoa	Francesco Famà	Site Investigator
Genoa	Elisabetta Capello	Site Investigator
Leipzig	Peter Schonknecht	Site PI
Leipzig	Ulrich Hegerl	Site Investigator
Leipzig	Tilman Hensch	Site Investigator
Leipzig	Martin Berwig	Site Investigator
Lille	Regis Bordet	Site PI
Lille	Florence Pasquier	Site Investigator
Lille	Stéphanie Bombois	Site Investigator
Lille	Marie-Anne Mackowiak	Site Investigator
Lille	Xavier Delbeuck	Site Investigator

Marseille	Mira Didic	Site PI
Marseille	Francesca de Anna	Site Investigator
Marseille	Jean-Philippe Ranjeva	Site Investigator
Naples	Andrea Soricelli	Site PI
Naples	Marco Salvatore	Site Investigator
Naples	Marco Aiello	Site Investigator
Perugia	Lucilla Parnetti	Site PI
Perugia	Lucia Farotti	Site Investigator
Perugia	Nicola Salvadori	Site Investigator
Perugia	Pietro Chiarini	Site Investigator
Perugia	Roberto Tarducci	Site Investigator
Perugia	Cinzia Costa	Site Investigator
Rome	Paolo Maria Rossini	Site PI
Rome	Camillo Marra	Site coPI
Rome	Pietro Spinelli	Site Investigator
Rome	Paola Chiovenda	Site Investigator
Rome	Valeria Guglielmi	Site Investigator
Rome	Giovanna Masone Iacobucci	Site Investigator
Rome/Chieti	Massimo Caulo	Site Investigator
Thessaloniki	Magda Tsolaki	Site PI
Thessaloniki	Antonis Drevelegas	Site Investigator
Toulouse	Pierre Payoux	Site PI

Toulouse	Helene Gros-Dagnac	Site Investigator

Figure legend.

Figure 1. Association between default mode network perfusion and AD features in MCI: APOE status (panel A), core pathophysiological (panel B) and neurodegenerative markers (panel C), cognitive (panel D), and vascular (panel E) features. Each dot represents a subject. Purple dots denote significant results. *p* denotes significance at the Fisher (*F*) test for the ANCOVA model (panel A) or the partial correlation test (panels B-E), set to 0.05. Degrees of freedom are reported in brackets.

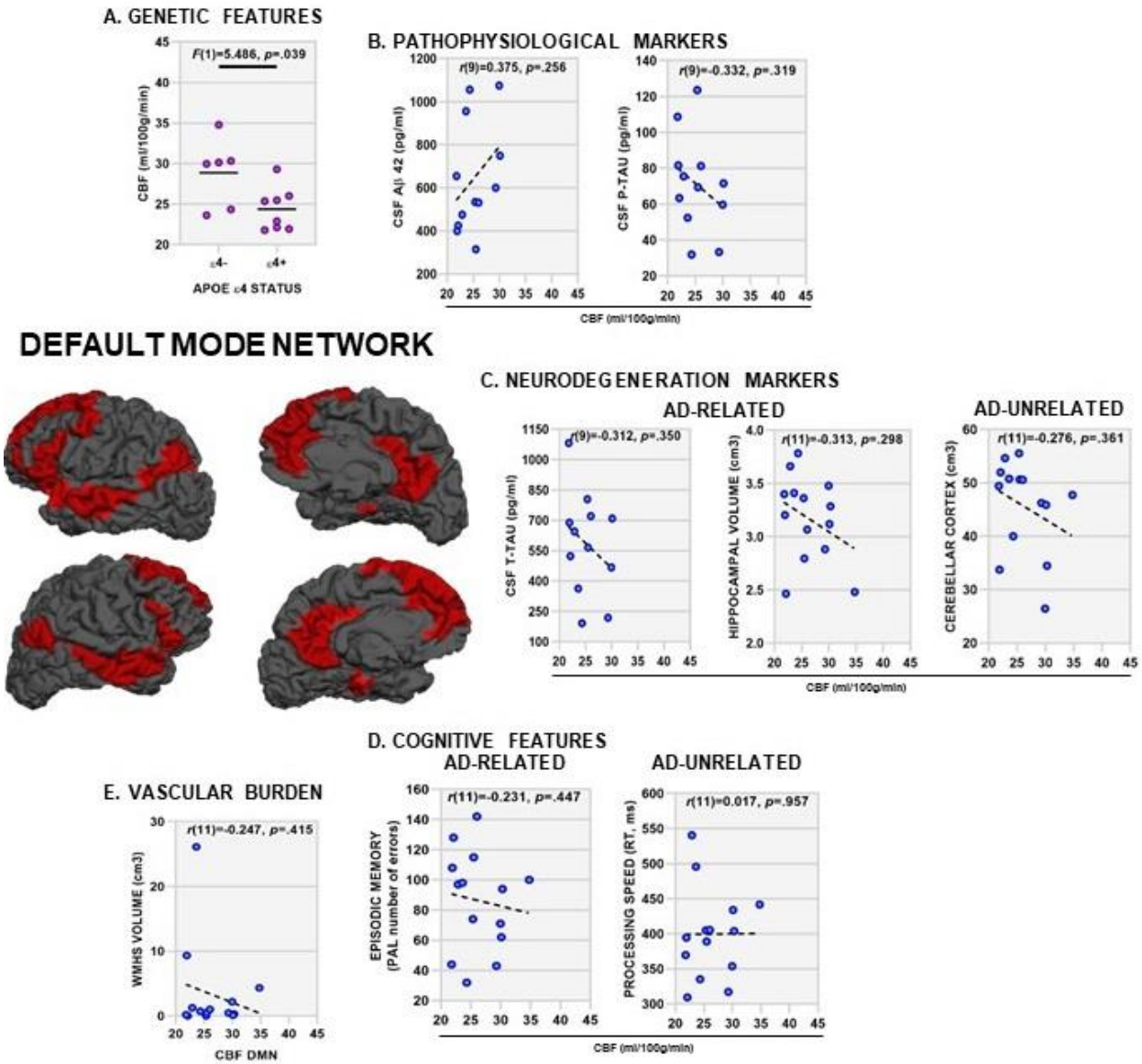

Abbreviations: ε4, allele 4 of the Apolipoprotein E gene; CBF, cerebral blood flow; CSF, cerebrospinal fluid; Aβ42, amyloid β peptide 1-42; t-tau, total tau protein; p-tau, phospho-tau

protein; PAL, paired associate learning test; RT, reaction time; WMHs, white matter hyperintensities; ml, milliliters; g, grams; min, minutes; pg/ml, picogram/milliliter; mm, millimeters; ms, milliseconds.

Figure 2. Association between limbic network perfusion and AD features in MCI: APOE status (panel A), core pathophysiological (panel B) and neurodegenerative markers (panel C), cognitive (panel D), and vascular features (panel E). Each dot represents a subject. Purple dots denote significant results. *p* denotes significance at Fisher (*F*) test for the ANCOVA model (panel A) or the partial correlation test (panels B-E), set to 0.05. Degrees of freedom are reported in brackets.

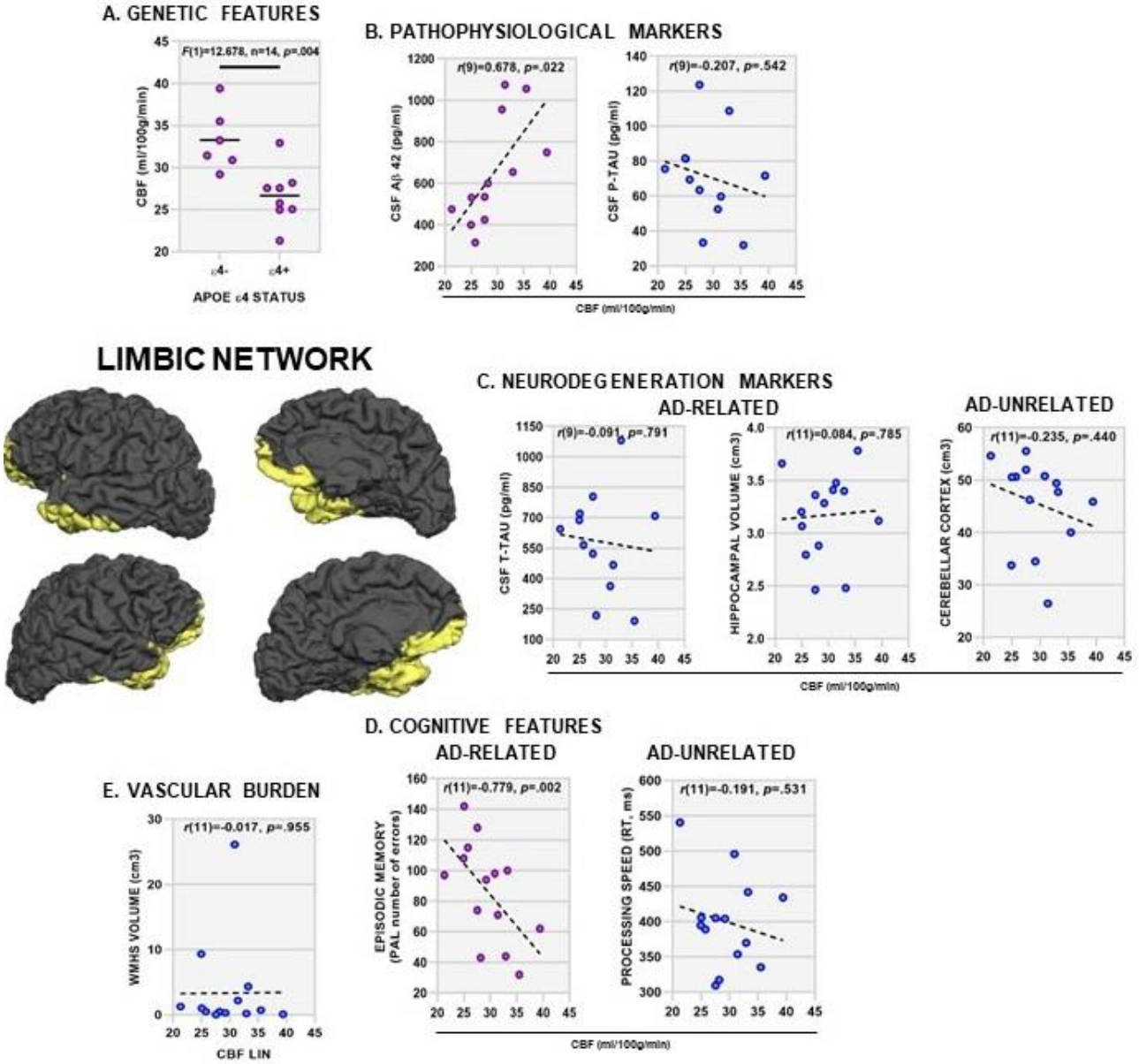

Abbreviations: ε4, allele 4 of the Apolipoprotein E gene; CBF, cerebral blood flow; CSF, cerebrospinal fluid; Aβ42, amyloid β peptide 1-42; t-tau, total tau protein; p-tau, phospho-tau

protein; PAL, paired associate learning test; RT, reaction time; WMHs, white matter hyperintensities; ml, milliliters; g, grams; min, minutes; pg/ml, picogram/milliliter; mm, millimeters; ms, milliseconds.

Supplementary Figure 1. Association between somatomotor network perfusion and AD features in MCI: APOE status (panel A), core pathophysiological (panel B) and neurodegenerative markers (panel C), cognitive (panel D), and vascular (panel E).features. Each dot represents a subject. *p* denotes significance at the Fisher (*F*) test for the ANCOVA model (panel A) or the partial correlation test (panels B-E), set to 0.05. Degrees of freedom are reported in brackets.

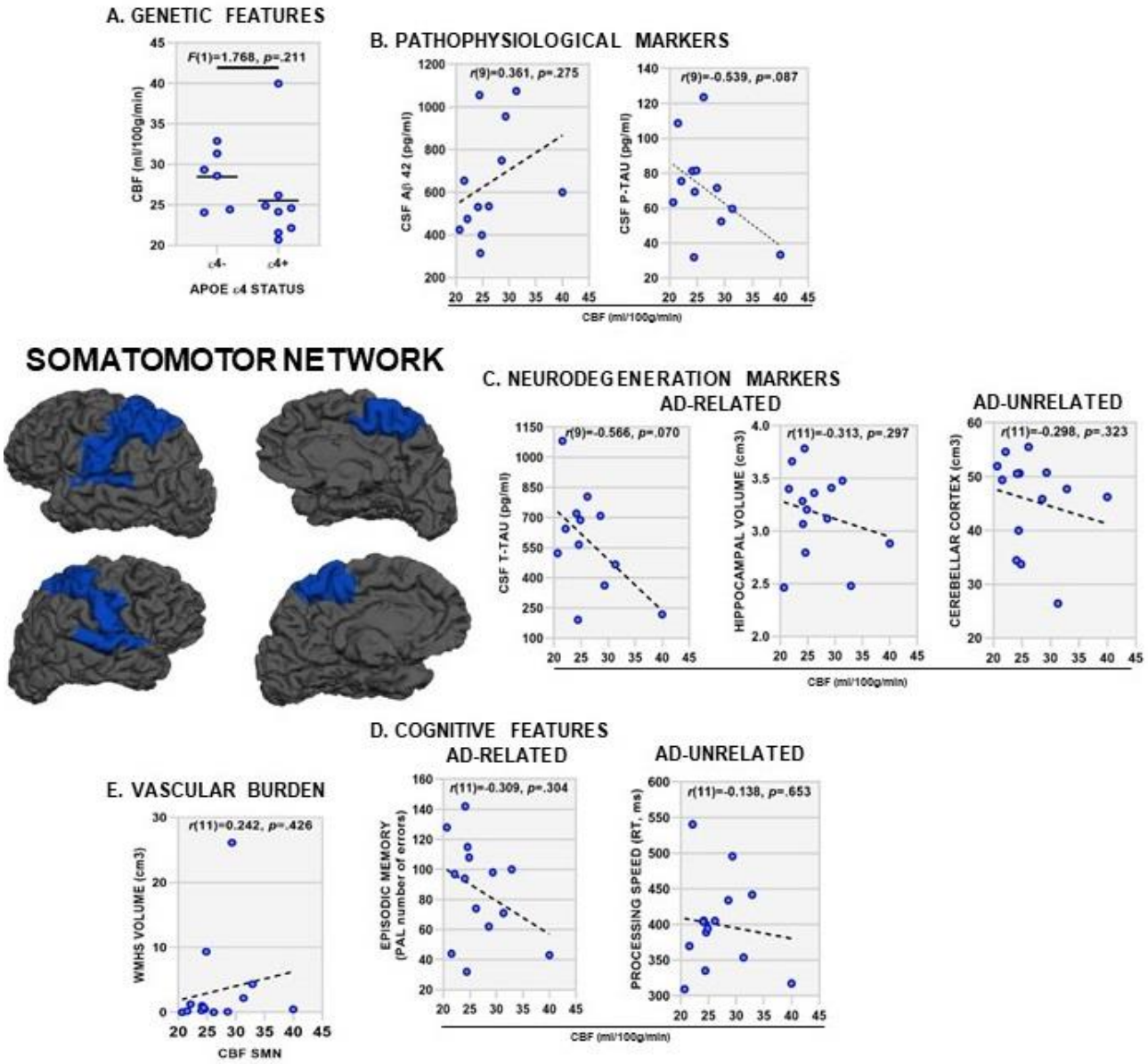

Abbreviations: ε4, allele 4 of the Apolipoprotein E gene; CBF, cerebral blood flow; CSF, cerebrospinal fluid; Aβ42, amyloid β peptide 1-42; t-tau, total tau protein; p-tau, phospho-tau protein; PAL, paired associate learning test; RT, reaction time; WMHs, white matter

hyperintensities; ml, milliliters; g, grams; min, minutes; pg/ml, picogram/milliliter; mm, millimeters; ms, milliseconds.

Supplementary Figure 2. Association between visual network perfusion and AD features in MCI: APOE status (panel A), core pathophysiological (panel B) and neurodegenerative markers (panel C), cognitive (panel D), and vascular (panel E) features. Each dot represents a subject. Purple dots denote significant results. *p* denotes significance at the Fisher (*F*) test for the ANCOVA model (panel A) or the partial correlation test (panels B-E), set to 0.05. Degrees of freedom are reported in brackets.

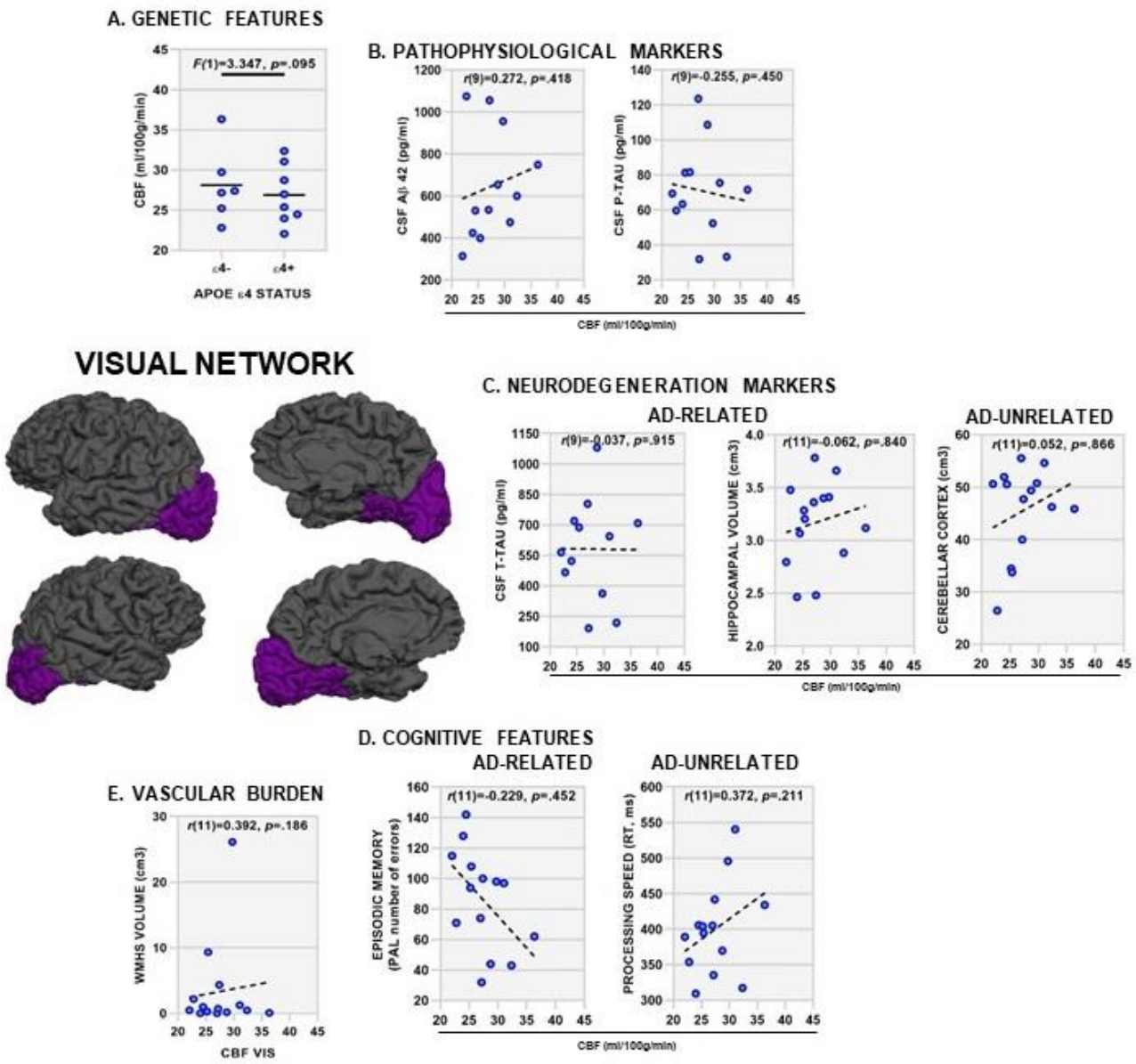

Abbreviations: Ɛ4, allele 4 of the Apolipoprotein E gene; CBF, cerebral blood flow; CSF, cerebrospinal fluid; Aβ42, amyloid β peptide 1-42; t-tau, total tau protein; p-tau, phospho-tau

protein; PAL, paired associate learning test; RT, reaction time; WMHs, white matter hyperintensities; ml, milliliters; g, grams; min, minutes; pg/ml, picogram/milliliter; mm, millimeters; ms, milliseconds.